Archive ouverte UNIGE
https://archive-ouverte.unige.ch

Article scientifique | Article | 2016

Accepted version | Open Access

This is an author manuscript post-peer-reviewing (accepted version) of the original publication. The layout of the published version may differ .

Rapid memory stabilization by transient theta coherence in the human medial temporal lobe

Thézé, Raphaël; Guggisberg, Adrian; Nahum, Louis; Schnider, Armin

How to cite

THÉZÉ, Raphaël et al. Rapid memory stabilization by transient theta coherence in the human medial temporal lobe. In: Hippocampus, 2016, vol. 26, p. 445–454. doi: 10.1002/hipo.22534

This publication URL: https://archive-ouverte.unige.ch/unige:79653
Publication DOI: 10.1002/hipo.22534

© This document is protected by copyright. Please refer to copyright holder(s) for terms of use.

HIPPOCAMPUS 00:00–00 (2015)

Rapid Memory Stabilization by Transient Theta Coherence in the Human Medial Temporal Lobe

Raphaël Thézé,[1,2] Adrian G. Guggisberg,[1,2] Louis Nahum,[1,2] and Armin Schnider[1,2]*

Abstract: Presenting stimuli again after presentation of intervening stimuli improves their retention, an effect known as the spacing effect. However, using event-related potentials (ERPs), we had observed that immediate, in comparison to spaced, repetition of pictures induced a positive frontal potential at 200–300 ms. This potential appeared to emanate from the left medial temporal lobe (MTL), a structure critical for memory consolidation. In this study, we tested the behavioral relevance of this signal and explored functional connectivity changes during picture repetition. We obtained high-density electroencephalographic recordings from 14 healthy subjects performing a continuous recognition task where pictures were either repeated immediately or after 9 intervening items. Conventional ERP analysis replicated the positive frontal potential emanating from the left MTL at 250–350 ms in response to immediately repeated stimuli. Connectivity analysis showed that this ERP was associated with increased coherence in the MTL region—left more that right—in the theta-band (3.5–7 Hz) 200–400 ms following immediate, but not spaced, repetition. This increase was stronger in subjects who better recognized immediately repeated stimuli after 30 min. These findings indicate that transient theta-band synchronization between the MTL and the rest of the brain at 200–400 ms reflects a memory stabilizing signal. © 2015 Wiley Periodicals, Inc.

KEY WORDS: consolidation; functional connectivity; inverse solution; spatio-temporal analysis; theta band

INTRODUCTION

Memory consolidation refers to the process by which a memory trace is stabilized over time (Nadel and Moscovitch, 1997). The medial temporal lobe (MTL) with the hippocampus plays a crucial role in this process (Squire et al., 2004).

How well information is retained critically depends on how it is presented. For instance, information is better retained in memory when it has been learned in well-separated presentations (spaced repetition) than in rapidly succeeding presentations (massed repetition). This encoding advantage has been first described by Ebbinghaus (1885) and is known as the spacing effect (SE; Greene, 1989). The underlying neural mechanisms are largely unknown. Studies using functional MRI showed that, the less brain activity decreased in response to rapidly repeated stimuli (weak priming effect, weak repetition suppression), the better subsequent retrieval of the repeated information was (Wagner et al., 2000; Xue et al., 2011). Similarly, the magnitude of connectivity in the MTL between learning sessions predicted resistance to forgetting (Vilberg and Davachi, 2013).

Compared with these studies, we made a seemingly paradoxical observation when healthy subjects performed a learning task in which some stimuli were immediately repeated, others after nine intervening items. As revealed by high-density event-related potentials (ERPs), immediately repeated stimuli, in comparison to new pictures and delayed repetitions, induced a frontal positivity at 200–300 ms, which appeared to reflect stronger left MTL activation as determined with inverse solutions (James et al., 2009). Intracerebral recordings in epileptic patients confirmed this localization (Nahum et al., 2011). The finding appeared paradoxical as it indicated particularly strong MTL activation during the processing of stimuli (immediate repetitions), which—over the whole group of subjects—are subsequently less well recognized than stimuli repeated after a delay. Nonetheless, the idea of a memory stabilizing effect of this signal obtained support from the observation that severely amnesic patients lack this signal (Nahum et al., 2014).

This study aimed to clarify the meaning of this early MTL signal by studying interregional interactions (synchronization) between brain regions (Friston, 2011) and by analyzing its behavioral effect. We used the same experimental paradigm as in our earlier study (James et al., 2009) and recorded brain activity with high-resolution electroencephalographic (EEG). We first replicated our earlier findings in a new group of subjects. We then determined coherence, a measure of the functional connectivity (FC) between brain regions (Guggisberg et al., 2011). We hypothesized that consolidation differences, as perceived with the SE, would be associated with a change in FC in a similar time frame (TF) as the ERP observed earlier and thus result from variations in the processing of immediately repeated items.

---

[1] **Division of Neurorehabilitation, Laboratory of Cognitive Neurorehabilitation, University Hospital, Geneva, Switzerland;** [2] **Department of Clinical Neurosciences, Laboratory of Cognitive Neurorehabilitation, University of Geneva, Switzerland**

Grant sponsor: Swiss National Science Foundation; Grant number: 32003B_155947.

***Correspondence to**: Prof. Armin Schnider, Service de Neuroréeducation, Hôpitaux Universitaires de Genève, 26, av. de Beau-Séjour, CH-1211 Geneva 14, Switzerland. E-mail: armin.schnider@hcuge.ch

Accepted for publication 16 September 2015.
DOI 10.1002/hipo.22534

Published online 00 Month 2015 in Wiley Online Library (wileyonlinelibrary.com).

© 2015 WILEY PERIODICALS, INC.

METHODS

Participants

Fifteen right-handed healthy subjects (9 women; age, 61.6 ± 10.2, 49 to 81) with no history of neurological or psychiatric illness gave written informed consent and were paid to take part in the study. All passed a brief neuropsychological evaluation and obtained normal values on the Mini Mental State Examination and various tests of episodic memory, working memory and executive functions. One subject was excluded from the analysis due to a high level of noise in the EEG data. All procedures were approved by the local Ethics Committee and conducted according to the Declaration of Helsinki.

Paradigm

Learning task

Subjects performed a continuous recognition task as described by James et al. (2009). It consisted of 120 black and white meaningful drawings (Snodgrass and Vanderwart, 1980). After the first presentation (New condition, $N = 120$), each item was repeated once, either immediately following a 2-s stimulus-free interval (One-Back condition, $N = 60$) or after nine intervening items (Ten-Back condition, $N = 60$). Subjects were asked to indicate whether they had already seen the same picture within the ongoing run. They pressed the left button of a response box with the right index to indicate "yes, I have seen it before" or the right button with the right middle finger to indicate "No, not seen before." Stimuli were presented for 1000 ms, at the size of 8° of visual angle, with an interstimulus interval of 2000 ms filled with a fixation cross.

Delayed recognition task

To test for the presence of a SE, participants performed a delayed recognition task 30 min after the initial recognition task. During this task, all 120 pictures from the learning task and 120 new pictures were presented in random order. Subjects had to indicate whether they had seen a picture in the previous learning task, or not, by pressing two different buttons with the right hand, as described in the learning task above.

The SE was calculated as:

$$\mathrm{SE} = (\mathrm{Hits}_{\text{Ten-Back}} - \mathrm{Hits}_{\text{One-Back}}) \times 100/60$$

where $\mathrm{Hits}_{\text{Ten-Back}}$ describes the number of correct recognitions in the delayed recognition task of items that had been repeated after nine intervening items in the learning task; $\mathrm{Hits}_{\text{One-Back}}$ describes the number of correct recognitions in the delayed recognition task of items that had been repeated immediately.

Data Acquisition

Recordings were done during the initial learning task and obtained with a 128-channel BioSemi ActiveTwo EEG system (BioSemi B.V., Amsterdam, The Netherlands) at a sampling rate of 512 Hz. The trials of each condition were aligned to the onset of visual stimulus presentation and epochs from 600 ms prestimulus to 1000 ms poststimulus onset were extracted. In addition to a criterion of +/−100 μV, artefacts such as blinks, eye movements, muscular contractions, or electrodes artefacts were excluded by visual inspection. Bad channels containing recurrent artefacts over prolonged periods were ignored from further analysis and interpolated from neighboring electrodes. Artefact-free epochs were rereferenced to the average of all nonexcluded channels

ERP Analysis

Spatio-temporal analysis

Similarly to James et al. (2009), and to replicate their findings, we applied a spatiotemporal segmentation to the ERPs recorded over the 128 electrodes between 0 and 600 ms poststimulus onset. Segments of stable electric field configurations (maps) were determined using an Atomize and Agglomerate Hierarchical Clustering analysis (Murray et al., 2008) in the group-averaged ERPs for each stimulus. The optimal number of cluster maps was determined by cross validation. The clusters identified on group-averaged ERPs were used to develop template maps to apply spatial correlation between them and between single-subjects ERPs. The output of this fitting was then used to analyze the strength of a map in a given condition and the interaction between maps and conditions in the time window where maps appeared visually different across conditions according to the cluster analysis of the grand-mean. Individual values of Global Explained Variance (GEV, measure of map dominance) and number of TF (measure of map duration) were subjected to repeated-measures ANOVA with map and experimental conditions (New, Ten-Back, and One-Back) as within-subject factors to verify whether the maps were statistically different in their respective conditions.

Waveform analysis

We tested the amplitude difference between conditions at the Fz electrode, as reported by James et al. (2009). We performed a repeated-measure ANOVA with the mean amplitudes over the period of interest determined by spatiotemporal segmentation as a within-subject factor.

Source analysis

A source estimation of intracranial generators was performed by applying a distributed linear inverse solution based on Local Auto-Regressive Average (LAURA) model using a 3D realistic head model with a solution space of 3005 nodes (Grave de Peralta Menendez et al., 2001; Grave de Peralta Menendez et al., 2004). Current distribution was calculated within the gray matter of the average brain provided by the Montreal Neurological Institute (MNI). To compare statistically the sources between conditions in the period of interest determined with the spatiotemporal segmentation, we computed the contrasts of local electrical current densities with time-point wise paired t-tests similar to statistical parametric mapping used in fMRI studies. Only periods for which $P < 0.01$ for at least 20 consecutive ms were retained.

FC Analysis

FC analysis was carried out in Matlab (The MathWorks, Natick) with NUTMEG (Dalal et al., 2011; http://www.nitrc.org/plugins/mwiki/index.php/nutmeg:MainPage) and its FC mapping toolbox (Guggisberg et al., 2011). For the localization of FC, we required an estimation of neural oscillations in the brain. To this end, we computed a lead-potential with 10 mm grid spacing using a similar spherical head model with anatomical constraints (Spinelli et al., 2000) based on the segmented gray matter of the MNI template brain. A scalar minimum variance beamformer was used to reconstruct grey matter oscillations from the surface EEG recordings (Sekihara et al., 2004). A fourth order Butterworth temporal bandpass filter between 3 and 45 Hz was applied to the recordings to optimize the beamformer for those frequencies (Dalal et al., 2008; Guggisberg et al., 2011). Adaptive spatial filter weights were calculated for each subject from all artefact-free epochs of a given condition in the bandwidth from 3 to 45 Hz, using the entire epoch duration.

EEG epochs were Fourier transformed using a sliding Hanning window of 300 ms width shifted in time steps of 50 ms. Fourier coefficients were projected to source space with the adaptive spatial filter. We could then compute the MSC between all gray matter voxel pairs. Coherence is usually calculated across multiple time windows. However, as we intended to investigate the time course of neural interactions in this study, we used an event-related approach (Andrew and Pfurtscheller, 1996) providing better time resolution. Event related coherence (ERCoh) between two Fourier transformed source time series X and Y was calculated across all K trials of a given condition, at each time window t, and in the frequency bands b theta (3–7.5 Hz), alpha (7.5–12.5 Hz), beta (12.5–30 Hz), and gamma (30–45 Hz):

$$ERCOh(b,t)=\frac{\left|\sum_{t\in B}\sum_{k\in K}X_k(f,t)Y_k{}^*(f,t)\right|^2}{\sum_{t\in B}\sum_{k\in K}|X_k(f,t)|^2\sum_{f\in B}\sum_{k\in K}|Y_k(f,t)|^2} \tag{1}$$

where f denotes the frequency bin, B the frequency bins corresponding to each band, and * the complex conjugate.

This resulted in a highly multidimensional data array (voxels × voxels × time window × frequency bands). To screen for relevant FC changes while avoiding false positives due to multiple testing, we proceeded as follows. First, we calculated the global FC of each voxel as the average ERCoh across its connections C with all other voxels:

$$\overline{ERCOh}=\tanh\left(\frac{1}{C}\sum_{C}\tanh^{-1}(ERCoh)\right) \tag{2}$$

Baseline ERCoh was calculated as the average of the time windows before presentation of the visual stimuli (-600 to -100 ms) and subtracted from all time windows. This served two purposes. First, it yielded event-related change of MSC during the encoding of the pictures. Second, it corrected for spatial leakage of the inverse solution, which would otherwise produce an overestimation and distortion of source MSC (Ghuman et al., 2011).

The resulting data matrix (voxels × time windows × frequency bands) was then subjected to a series of statistical tests.

We tested whether ERCoh changes in each condition were different from zero with t-tests for one sample. Then, we performed a paired comparison of the One-Back and Ten-Back conditions to highlight significant differences between them. Third, we evaluated whether ERCoh changes were associated with behavioral differences. To this end, subjects were dichotomized according to their delayed recognition performance in the post-test using a median split. We then tested whether good performers had different ERCoh changes than bad performers using an unpaired t-test.

Each of these tests was computed multiple times at each voxel, time window and frequency band. We used a pragmatic approach to correct for the family wise error, which consisted in combining these statistical tests such that only voxels, time windows, and frequency bands, which were significant at level $P < 0.05$ (uncorrected) in all of them would be above threshold. This resulted in new binary maps named "conjunction maps" in which the entry 1 indicated voxels, time windows and frequency bands, which were significant in all statistical tests; the entry 0 indicated all other elements. According to our hypothesis, we expect neural mechanisms of encoding that are specific to either the One-Back or the Ten-Back condition, hence providing a possible explanation for the SE. The conjunction map therefore had to fulfill all following conditions:

1. ERCoh changes are different from zero in the condition of interest ($P < 0.05$)
2. ERCoh changes are different in the One-Back than/as compared with the Ten-Back condition ($P < 0.05$)
3. Subjects with good recognition in the post-test have different ERCoh changes than bad performers ($P < 0.05$).

In addition, we also looked for ERCoh changes related to memory encoding, which were common to both immediate and delayed repetition. The conjunction map for neural mechanisms of encoding in both conditions had to survive all following tests:

1. ERCoh changes are different from zero in both the the One-Back and Ten-Back condition ($P < 0.05$)
2. Subjects with good recognition in the post-test have different ERCoh changes than bad performers ($P < 0.05$).

To remove changes at single voxels which are unlikely of physiological origin, we additionally required a significant cluster of at least 10 consecutive voxels.

We then performed permutation tests to evaluate the probability that significant elements in these conjunction maps are false positives. At each of 2000 permutations, we first inverted the polarity of the ERCoh change values for some subjects (i.e., we multiplied the values at all voxels, time windows, and frequency bands by -1), with a different combination of inverted subjects in each permutation. New conjunction maps were then computed from the permutated dataset. The proportion of

TABLE 1.

Behavioral Scores

	Learning		Post	
	Correct (%)	RT (ms)	Correct (%)	RT (ms)
New	96 ± 3	991 ± 327	87 ± 24	1160 ± 559
One-Back	98 ± 3	850 ± 142	75 ± 15	1046 ± 293
Ten-Back	94 ± 8	973 ± 167	87 ± 12	986 ± 205

Average correct answers (Hits) in percentage and RT in ms of all subjects in each condition for both learning and delayed task.

permutations in which we observed any significant voxel, at any time window and frequency band was then used as probability that the observed changes were due to pure chance. By scanning all voxels, time windows, and frequency bands at each permutation, we effectively controlled for multiple testing.

We defined regions of interest (ROIs) as significant contiguous voxels in the conjunction maps and computed the mean ERCoh change across its voxels. Finally, we defined the ROIs as seed area and analyzed ERCoh to each other voxel.

Association Between ERP and Coherence

To further understand the relationship between FC and ERPs, we calculated Pearson correlation between ERCoh change and ERP current amplitude in the MTL in the One-Back condition. Coherence change and ERP amplitude were each calculated as the average across significant time points and voxels in the MTL. Both values were computed in source space, that is, after projection of sensor data to the brain with the inverse solution. Each subject was thus attributed one value for the average ERCoh change from baseline and another for the average amplitude of the ERP in the One-Back condition, and the Pearson correlation coefficient was computed between these values. The same calculation was applied between the ERP current amplitude in the MTL and the ERCoh change from baseline in the right parietal cortex, as well as ERCoh changes in an equidistant control region, the right superior medial frontal gyrus.

RESULTS

Behavioral Analyses

Spacing effect

As expected, a SE was found (Table 1). Participants better recognized Ten-Back items (mean hit rate ± standard error, 86.6 ± 11.7%) than One-Back items (75.2 ± 15.4%) in the delayed recognition test ($t(13) = -6.55$, $P < 0.001$). Reaction Times (RT) indicate that there is no overlap between the timing of the button press and the effect of interest (Table 1).

The SE negatively correlated with correct delayed recognition of One-Back stimuli from the initial learning task: subjects showing a higher SE had significantly poorer delayed recognition of One-Back stimuli (Fig. 1A; $r = -0.77$, $P = 0.0021$). There was no such association for the Ten-Back stimuli (Fig. 1B, $r = -0.19$, $P = 0.54$). Delayed recognition of One-Back items and Ten-Back items correlated (Fig. 1C) in the task ($r = 0.77$, $P = 0.002$). One subject (marked as an X) was ignored for these correlations due to considerable differences of performance from the group, but was included in the other calculations because a consolidation process is nevertheless occurring (i.e., overall performance is low but SE taking place).

Age effects

There was no significant age difference between high performers (mean = 65.83 years ± 10.44) and low performers (mean = 58.4 years ± 9.33) ($t(12) = 1.41$, $P = 0.18$) in the delayed recognition task. Moreover, age was not correlated with the number of hits, neither on One-Back stimuli ($r = 0.23$, $P = 0.43$), nor on Ten-Back stimuli ($r = 0.28$, $P = 0.33$). Finally, there was no association between age and the SE ($r = -0.045$, $P = 0.88$).

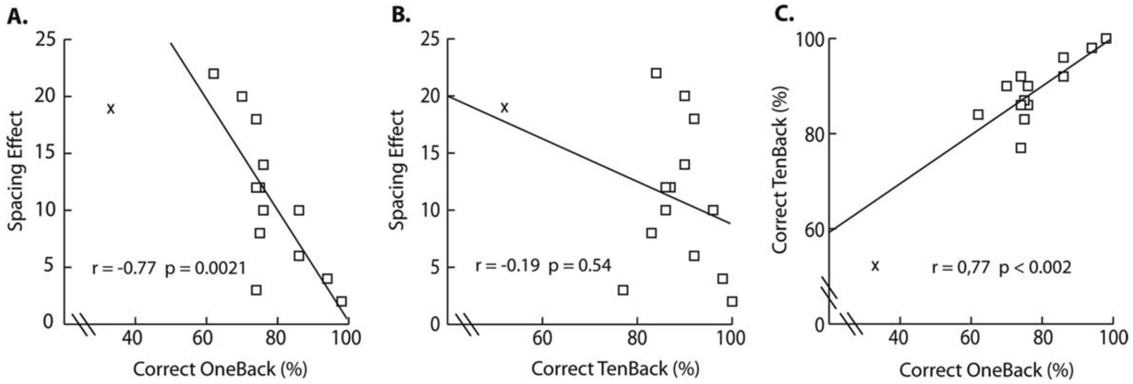

FIGURE 1. Behavioral correlations: Correlation between Spacing Effect and (A) correct recognition of OneBack items after 30 minutes, (B) recognition of TenBack items after 30 minutes; (C) correlation between recognition of OneBack and TenBack items after 30 minutes. Subject 7 (marked with an x) was ignored as an outlier for calculation of correlation coefficients.

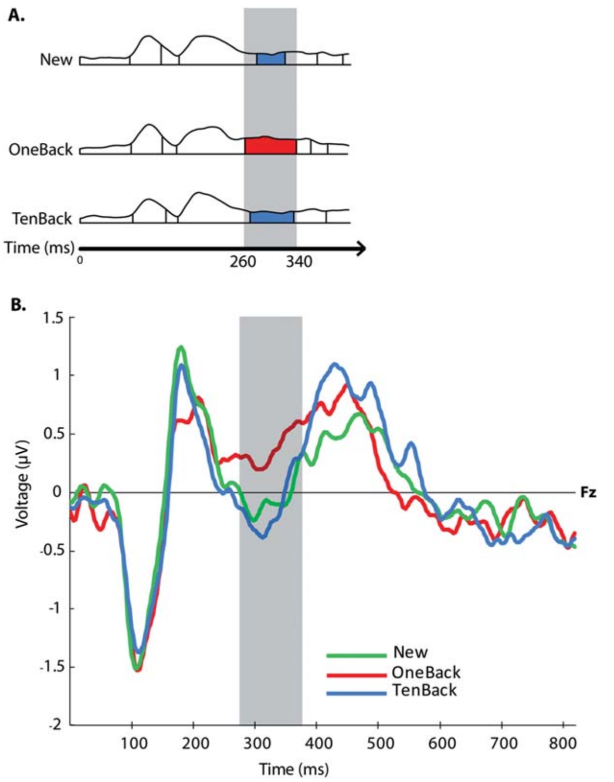

FIGURE 2. Spatio-temporal analysis: (A) Segmentation procedure of group averaged ERPs for each condition. The colored segments correspond to different topographical configurations of potential distribution at the scalp. (B) Waveform analysis at electrode Fz in response the New, One-Back, and Ten-Back stimulus during the learning task. The area delimited in grey is the period of interest displaying significant amplitude difference between One-Back and Ten-Back conditions. [Color figure can be viewed in the online issue, which is available at wileyonlinelibrary.com.]

ERP Analysis

Spatio-temporal analysis

Similar to James et al. (2009), spatiotemporal segmentation confirmed the existence of a distinct map for One-Back items in the learning task (Map 5, Fig. 2A), with a different configuration than New and Ten-Back items (Map 6), during a similar time period, that is, between approximately 260 and 340 ms (Fig. 2A). Those maps were statistically tested for differences in number of TF and GEV and revealed a significant interaction between maps and conditions during the period of interest (GEV: $F(2, 26) = 4$, $P = 0.029$; TF: $F(2, 26) = 7$, $P = 0.004$); Map 5 both explained more variance and was more present in the One-Back condition than in the two other conditions (New and Ten-Back).

Waveform analysis

There was a strong positive potential wave over the Fz electrode between 256 and 336 ms in response to One-Back items as opposed to the other two conditions (Fig. 2B). This difference was statistically significant (F (2, 26) = 4.16, $P = 0.027$).

Source analysis

Source estimation performed over the time period of the differences observed in the spatio-temporal and waveform analyses indicated a difference of electrical current densities between One-Back items on one side and New or Ten-Back items. One-Back items displayed stronger activity ($P < 0.01$) in the left MTL and frontal limbic area (Figs. 3A,B) compared with the two other conditions.

Functional Connectivity

Conjunction analysis

We first screened the multidimensional dataset for network correlates of encoding using the conjunction maps. In the One-Back condition of the learning task, the conjunction map was significant in the theta frequency band (3–7.5 Hz) between 200 and 400 ms after stimulus presentation in the parahippocampal region (Fig. 4A). This indicates that, in comparison to baseline, voxels in the parahippocampal region significantly increased coherence to all other cortical voxels in the One-Back condition ($t(13) = 3.44$, $P = 0.0044$, uncorrected). This theta–band ERCoh increase was significantly greater than ERCoh changes induced by the Ten-Back items ($t(13) = 2.38$, $P = 0.033$, uncorrected; Fig. 4C). In addition, subjects obtaining high scores in the delayed recognition task showed greater theta-band connectivity than subjects with a lower performance ($t(12) = 2.8$, $P = 0.017$, uncorrected; Fig. 4E).

No significant elements were found in the conjunction map of the Ten-Back condition. Conjunction screening for common

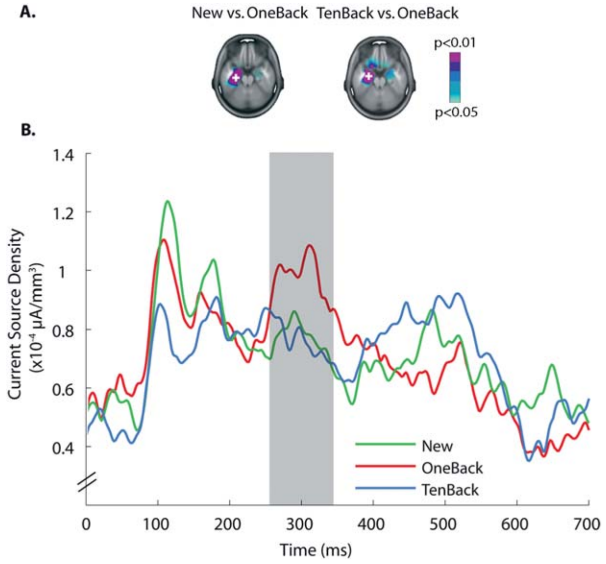

FIGURE 3. Source estimations: (A) time-point wise paired t-tests in source space to compare statistically the brain activation between conditions in the period of interest determined with the spatiotemporal segmentation. The region of interest within the MTL is indicated by a white cross in axial view. (B) Local variations of electrical current densities at the region of interest. [Color figure can be viewed in the online issue, which is available at wileyonlinelibrary.com.]

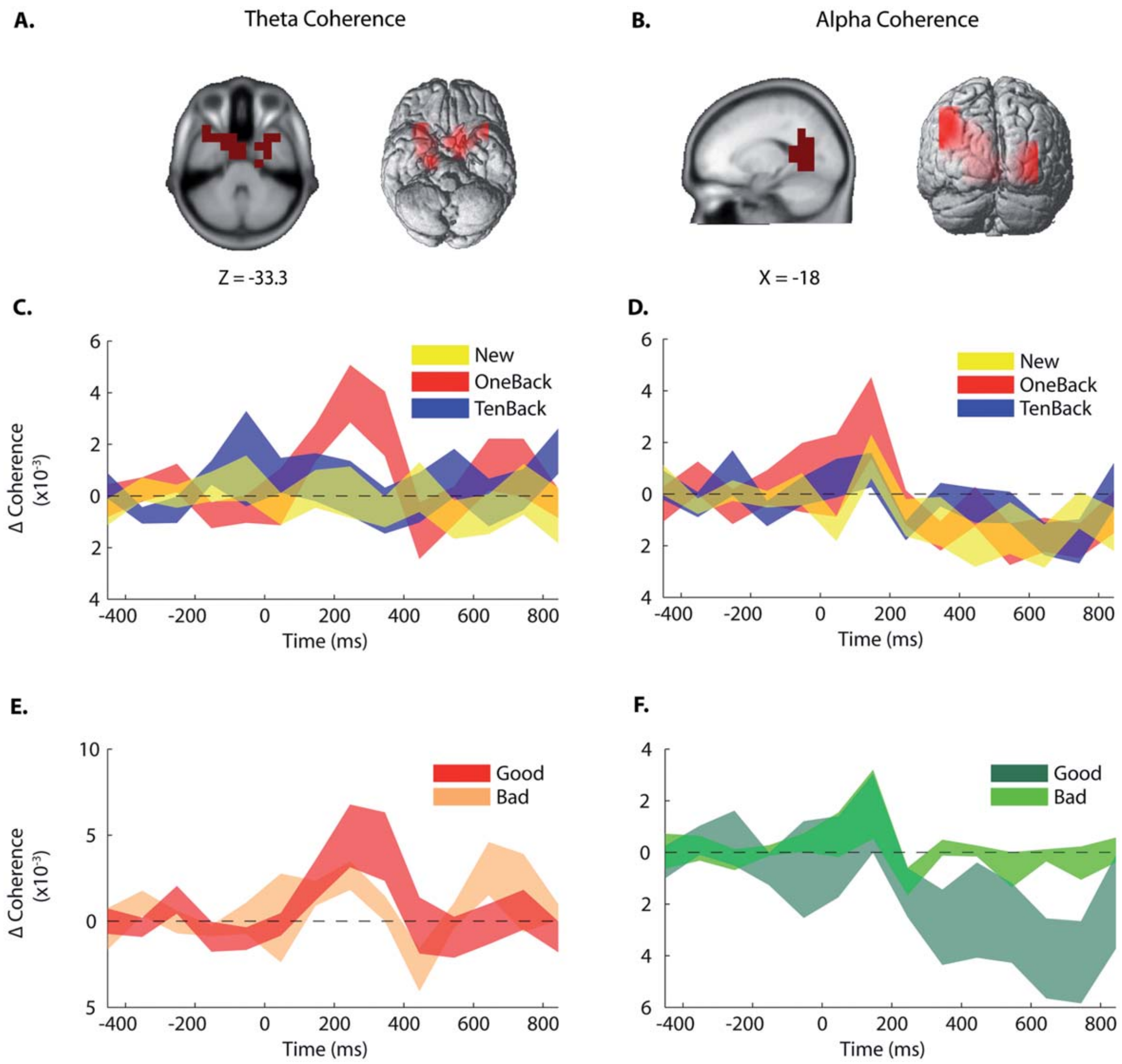

FIGURE 4. **Average coherence change: Region of significant coherence change in (A) the para-hippocampal region and (B) the retrosplenial cortex. Average event-related coherence (ERCoh) change between (C) parahippocampal region, or (D) the retrosplenial cortex, and the rest of the brain for all subjects in all conditions. Average ERCoh change upon segregation of good vs. bad performers in (E) the parahippocampal region for the One-Back condition and (F) the retrosplenial cortex for all conditions. [Color figure can be viewed in the online issue, which is available at wileyonlinelibrary.com.]**

correlates in One-Back and Ten-Back conditions revealed a significant area in the retrosplenial cingulate gyrus between 500 and 800 ms in the alpha-band (Fig. 4B). This indicates that significant ERCoh decrease occurred between this area and the rest of the brain in both the One-Back and Ten-Back conditions ($t(13) = -2.86$, $P = 0.013$, uncorrected; Fig. 4D) and was associated with good picture recognition in the post-test. Subjects with greater disconnection showed higher percentage of correct answers, whereas subjects with little or no change in connectivity obtained lower percentage of correct responses ($t(12) > 2.8$, $P < 0.016$, uncorrected; Fig. 4F).

We verified the probability of finding significant elements in the conjunction maps due to pure chance. The proportion of permutations in which we observed any significant voxel, at any time window and frequency band, was 0.039 for the One-Back condition-specific map and 0.075 for the common map. This demonstrates that the risk for false positive findings in our conjunction maps was low.

Seed analysis

We then defined the parahippocampal region as a seed region for calculating the ERCoh to each other voxel (Fig. 5A). A significant coherence increase ($t(13) = 2.72$, $P < 0.018$, uncorrected) from baseline was observed in the theta frequency band between the parahippocampal region and the right inferior parietal area in the period from 200 to 400 ms after stimulus onset (Fig. 5B). The coherence increase was significantly

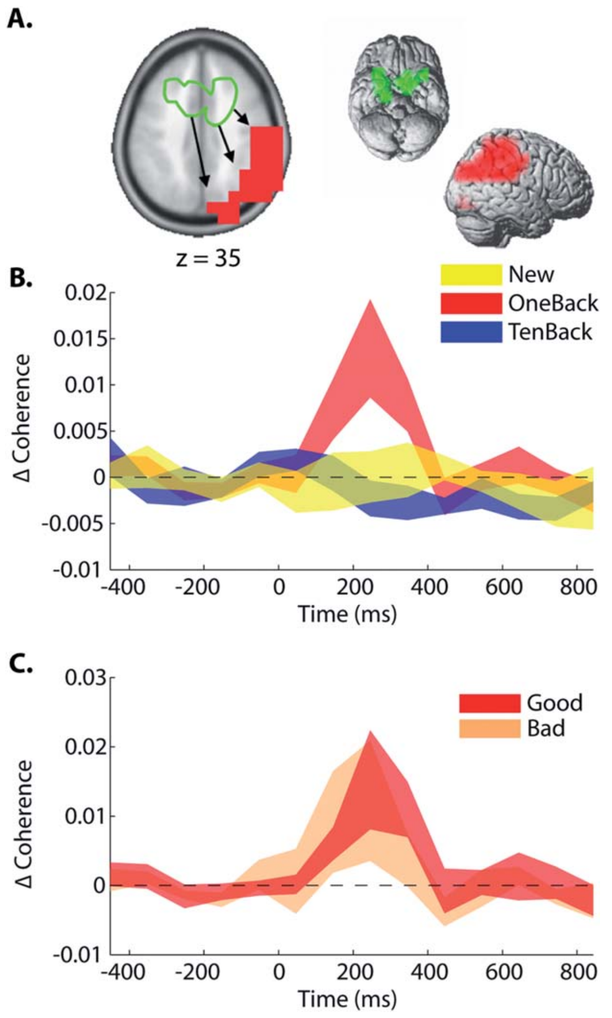

FIGURE 5. Average coherence change seeded in the parahippocampal region: Region of significant coherence change between the parahippocampal region (represented with green delineation) and the inferior parietal lobe (red area) in axial view segmented at the slice associated with parietal activation (A). Average ERCoh change between seed region and the parietal region for all subjects in all conditions (B). Average ERCoh change upon segregation of good vs. bad performers between the two regions (C). [Color figure can be viewed in the online issue, which is available at wileyonlinelibrary.com.]

greater in the One-Back than in the Ten-Back condition ($t(13) = 3.6$, $P = 0.003$, uncorrected). However, the difference between high and low performers was not significant ($t(12) = 1.28$, $P = 0.22$, uncorrected; Fig. 5C).

Segregation of subjects according to their performance showed only a significant increase of coherence between the seed region and the surrounding areas.

Power

Coherence, as measured in this study, reflects synchronized oscillations from the region of interest with the rest of the brain. By contrast, power reflects the amplitude of oscillations in a given frequency in local population of neurons. Using a similar approach as Van Strien et al. (2007), we found a significant increase in theta power in parahippocampal regions over the whole period post-stimulus (Fig. 6A). However, unlike the coherence increase, this power increase was not specific to the One-Back condition. In fact, we found no significant difference across each of the time windows between One-back and Ten-Back conditions. Furthermore, the power increase lasted longer than the coherence increase.

The decrease in alpha-band coherence in the posterior cingulum occurred without corresponding change in alpha power ($P > 0.05$; Fig. 6B).

Association Between ERP and Coherence

The increase of theta-band coherence between the MTL and the rest of the brain in the One-Back condition correlated significantly with the corresponding current amplitude of the source signal of the ERP in the MTL ($r = 0.6$, $P = 0.025$; Fig. 7A). This correlation was specific to the time window between 200 and 400 ms after stimulus presentation identified in our previous analyses. The very same correlation coefficient was found between the ERP amplitude in MTL and ERCoh changes in the right parietal cortex (Fig. 7B), but not for control regions—here the right superior medial frontal gyrus—which did not correlate with ERP from the MTL (Fig. 7C).

DISCUSSION

This study confirms in a new group of participants the presence of a distinct positive frontal potential in response to

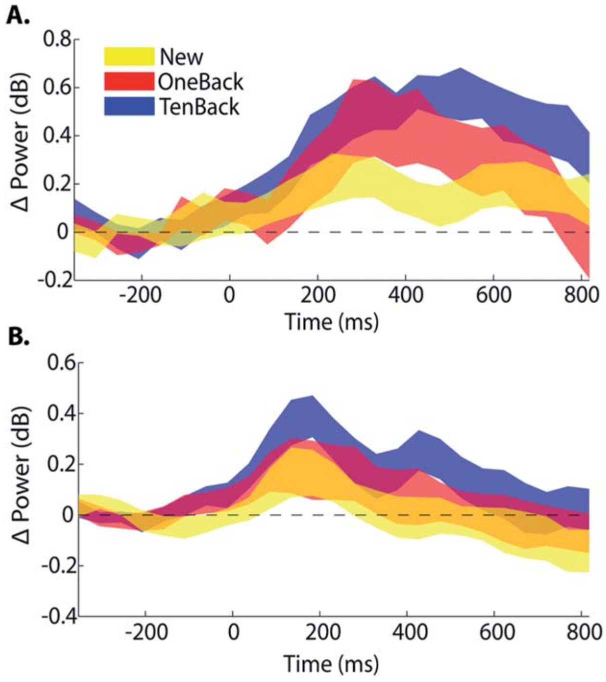

FIGURE 6. Power change: Theta power change in the MTL (A) and alpha power change in the retrospenial cortex (B). [Color figure can be viewed in the online issue, which is available at wileyonlinelibrary.com.]

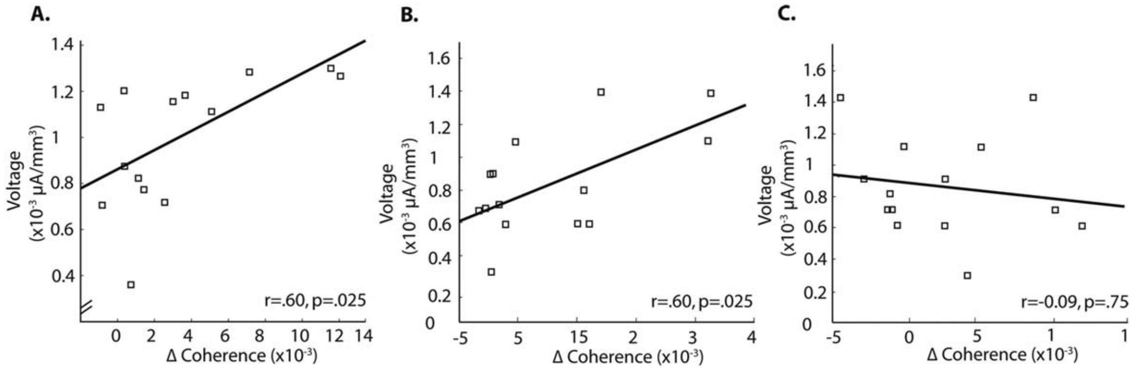

FIGURE 7. Neural correlates: (A) Correlation between ERCoh change and ERP amplitude at the MTL in the One-Back condition. (B) Correlation between ERCoh change in the right parietal cortex and ERP amplitude at the MTL in the One-Back condition. (C) Correlation between ERCoh change in the right superior medial frontal gyrus and ERP amplitude at the MTL in the One-Back condition.

immediately repeated visual stimuli, similar to earlier observations (Kim et al., 2001; Van Strien et al., 2007; James et al., 2009). Inverse solution analysis again localized the source of this potential in the MTL. Most importantly, the present study sheds light on the functional significance of this signal and of the involved network. We found that immediate stimulus repetitions induced a transient increase of coherence in the MTL, which was associated with stabilization of the memory trace. This increase of FC between the MTL and the rest of the brain was specific for immediate repetition (in comparison to new stimuli and spaced repetition) and distinct in time (200–400 ms), topography (MTL, left more than right), and frequency (theta range, 3.5–7 Hz).

The results add new, independent evidence to the idea that the MTL is involved in the early phase of processing of immediate stimulus repetitions. Our earlier study (James et al., 2009) had indicated activity in the left hippocampal area about 200–350 ms after immediate stimulus repetition. Depth electrode recordings confirmed this anatomical interpretation (Nahum et al., 2011). The present study not only used a different method, independent of the ERP analyses used in the earlier study, but also involved a different group of subjects. This result is entirely compatible with the ERP analysis, although laterality was less pronounced. Together, these results indicate that the MTL emits a transient signal in the theta range upon immediate stimulus presentation.

Whether this signal reflects detrimental interference with ongoing MTL activity or an MTL signal protecting against interference, has been unclear. MTL activity has rarely been studied during short-term memory tasks. Activation has been observed during retention of spatial relations between items (Hannula and Ranganath, 2008) or the active maintenance of faces (Ranganath and D'Esposito, 2001). However, fMRI as used in these studies has low temporal resolution, making it impossible to attribute such observations to a precise processing stage. In any case, this study indicates that the early MTL signal is protective for the memory trace: subjects having stronger MTL coherence upon immediate repetition performed better overall, but particularly with regards to late recognition of immediately repeated stimuli. Incidentally, these subjects then had a weaker measurable SE.

The coherence increase specifically concerned the theta band. The results bears superficial resemblance to Van Strien et al. (2007) who reported greater theta band power (4–6 Hz) from 250 to 625 ms interval upon immediate repetition of words. However, theta power, as determined in the study by Van Strien et al. (2007) reflects the amplitude of oscillations in a given frequency in populations of neurons rather than synchronized oscillations of a region of interest with the rest of the brain, as reflected in the coherence measure used here. In our study, we also found increased theta power, but in response to all stimuli. Thus, it appears that it is the coherence change, rather than power increase, which is specifically related to memory encoding upon immediate repetition.

Theta oscillations are thought to be induced by interactions within neuronal networks, notably pyramidal cells of the hippocampus (Miller, 1991). Theta activity in neo-cortical regions could reflect cortico-hippocampal feedback loops (Klimesch, 1999). In humans, theta oscillations have previously been described in association with working memory load during the maintenance of visual scenes (Klimesch et al., 1997; Sauseng et al., 2005; Raghavachari et al., 2006; Fuentemilla et al., 2010), the memorization of sequences of digits (Jensen and Tesche, 2002), and mental manipulation of learned patterns (Sauseng et al., 2005). Animal studies suggested a role for increased theta activity in long-term memory encoding. Theta coherence between hippocampus and cortical areas was increased as animals reliably acquired a rule providing them reward (Benchenane et al., 2010; Brincat and Miller, 2015). These findings support a role of transient theta coherence also for human long-term memory: the stabilization of information held in working memory.

The increase in MTL theta coherence, similar to the effects in the conventional ERP analysis, was specific for immediately repeated stimuli. Indeed, immediately repeated stimuli are known to induce particularly strong ERP effects (Kim et al., 2001; Van Strien et al., 2007); a stimulus repeated after only one interposed stimulus induces an ERP similar to a stimulus repeated after 32 intervening stimuli (Friedman, 1990a,b). From the electrophysiological perspective, the SE is reflected in the fact that stimuli repeated after intervening stimuli—in contrast to immediately repeated stimuli—are treated very similarly as new stimuli, that is, as if they were a new event. Immediate repetition as tested here is, of course, an extreme form of massed learning. Our results, therefore, may not apply to all types of SEs. Nonetheless, within the limits of the paradigm, they suggest that the SE, while beneficial for anyone, may have relatively little importance for very "rapid memory encoders," while it is crucial for the functioning of "slow memory encoders." Our study shows that subjects having a transient increase of MTL coherence upon immediate repetition can largely compensate for the disadvantage of massed learning.

Although the theta coherence increase was specifically localized in the MTL (similar to the conventional ERP analyses) this area did not act in isolation. We observed that the MTL had coherent activity with the parietal region at 200–400 ms. Furthermore, the coherent activity of both aforementioned regions similarly correlates with the ERP amplitude at the left MTL. The same was not true for the right superior medial frontal gyrus, analyzed as a control region. The observation underscores the spatial specificity of the coherence. The parietal lobes have repeatedly been linked to memory functions (Cabeza et al., 2008). In this study, coherence in the parietal area did not predict performance. This is compatible with studies attributing to the parietal lobes a more general role for memory: the involvement in a memory retrieval-related network linked to successful recollection (Vilberg and Rugg, 2008), or successful maintenance of items in short-term memory (Sauseng et al., 2009).

In addition to this signature of encoding upon immediate repetition, we observed a decrease in retrosplenial alpha-band coherence that was generally associated with encoding performance, independently of condition. While unexpected, this finding is not irrelevant as the retrosplenial cortex and the parahippocampal areas are heavily interconnected (Suzuki and Amaral, 1994; Selden et al., 1998). A lesion of the retrosplenial cortex can produce retrograde and anterograde amnesia in humans (Valenstein et al., 1987; Masuo et al., 1999). Consistent with its known involvement in memory systems (Fletcher et al., 1995b), our finding also relate to the hypothesis that the precuneus is involved in conscious memory recall during visual imagery (Fletcher et al., 1995a). We suggest that a relative isolation of this area from alpha-band interactions might contribute to successful encoding.

In summary, this study confirms the appearance of an early EEG signal in response to immediately repeated stimuli, which appears to emanate from the MTL and has the following characteristics: it is associated with improved later recognition of the presented items (this study), is absent in severely amnesic subjects (Nahum et al., 2014) is expressed by a frontal positivity at 200–300 ms in waveform analysis (James et al., 2009), and corresponds to a coherence increase of the MTL in the theta band. Depth electrode recordings also indicated a hippocampal source (Nahum et al., 2011). The study indicates that theta coherence is involved in rapid memory stabilization. More generally, this signal appears to have the necessary qualities to serve as an electrophysiological marker of the MTL's intervention in rapid memory stabilization.

REFERENCES

Andrew C, Pfurtscheller G. 1996. Event-related coherence as a tool for studying dynamic interaction of brain regions. Electroencephalogr Clin Neurophysiol 98:144–148.

Benchenane K, Peyrache A, Khamassi M, Tierney PL, Gioanni Y, Battaglia FP, Wiener SI. 2010. Coherent theta oscillations and reorganization of spike timing in the hippocampal-prefrontal network upon learning. Neuron 66:921–936.

Brincat SL, Miller EK. 2015. Frequency-specific hippocampal-prefrontal interactions during associative learning. Nat Neurosci 18:576–581.

Cabeza R, Ciaramelli E, Olson IR, Moscovitch M. 2008. The parietal cortex and episodic memory: An attentional account. Nat Rev. Neurosci. 9:613–625.

Dalal SS, Guggisberg AG, Edwards E, Sekihara K, Findlay AM, Canolty RT, Berger MS, Knight RT, Barbaro NM, Kirsch HE, Nagarajan SS. 2008. Five-dimensional neuroimaging: Localization of the time-frequency dynamics of cortical activity. Neuroimage 40:1686–1700.

Dalal SS, Zumer JM, Guggisberg AG, Trumpis M, Wong DD, Sekihara K, Nagarajan SS. 2011. MEG/EEG source reconstruction, statistical evaluation, and visualization with NUTMEG. Comput Intell Neurosci 2011:758973-

Ebbinghaus H. 1885. Über das Gedächtnis: Untersuchungen zur experimentellen Psychologie. Leipzig: Duncker & Humblot.

Fletcher P, Frith C, Baker S, Shallice T, Frackowiak R, Dolan R. 1995a. The mind's eye—precuneus activation in memory-related imagery. Neuroimage 2:195–200.

Fletcher PC, Frith CD, Grasby PM, Shallice T, Frackowiak RS, Dolan RJ. 1995b. Brain systems for encoding and retrieval of auditory-verbal memory. An in vivo study in humans. Brain 118 (Pt 2):401–416.

Friedman D. 1990a. Cognitive event-related potential components during continuous recognition memory for pictures. Psychophysiology 27:136–148.

Friedman D. 1990b. ERPs during continuous recognition memory for words. Biol Psychol 30:61–87.

Friston K. 2011. Dynamic causal modeling and Granger causality Comments on: The identification of interacting networks in the brain using fMRI: model selection, causality and deconvolution. Neuroimage 58:303–305. author reply 310-1.

Fuentemilla L, Penny WD, Cashdollar N, Bunzeck N, Duzel E. 2010. Theta-coupled periodic replay in working memory. Curr Biol 20: 606–612.

Ghuman AS, McDaniel JR, Martin A. 2011. A wavelet-based method for measuring the oscillatory dynamics of resting-state functional connectivity in MEG. Neuroimage 56:69–77.

Grave de Peralta Menendez R, Gonzalez Andino S, Lantz G, Michel CM, Landis T. 2001. Noninvasive localization of electromagnetic epileptic activity. I. Method descriptions and simulations. Brain Topogr 14:131–137.

Grave de Peralta Menendez R, Murray MM, Michel CM, Martuzzi R, Gonzalez Andino SL. 2004. Electrical neuroimaging based on biophysical constraints. Neuroimage 21:527–539.

Greene RL. 1989. Spacing effects in memory: Evidence for a two-process account. J Exp Psychol 15:371-

Guggisberg AG, Dalal SS, Zumer JM, Wong DD, Dubovik S, Michel CM, Schnider A. 2011. Localization of cortico-peripheral coherence with electroencephalography. Neuroimage 57:1348–1357.

Hannula DE, Ranganath C. 2008. Medial temporal lobe activity predicts successful relational memory binding. J Neurosci 28:116–124.

James C, Morand S, Barcellona-Lehmann S, Michel CM, Schnider A. 2009. Neural transition from short- to long-term memory and the medial temporal lobe: A human evoked-potential study. Hippocampus 19:371–378.

Jensen O, Tesche CD. 2002. Frontal theta activity in humans increases with memory load in a working memory task. Eur J Neurosci 15: 1395–1399.

Kim M-S, Kim J-J, Kwon JS. 2001. The effect of immediate and delayed word repetition on event-related potential in a continuous recognition task. Cogn Brain Res 11:387–396.

Klimesch W. 1999. EEG alpha and theta oscillations reflect cognitive and memory performance: A review and analysis. Brain Res Rev 29:169–195.

Klimesch W, Doppelmayr M, Schimke H, Ripper B. 1997. Theta synchronization and alpha desynchronization in a memory task. Psychophysiology 34:169–176.

Masuo O, Maeshima S, Kubo K, Terada T, Nakai K, Itakura T, Komai N. 1999. A case of amnestic syndrome caused by a subcortical haematoma in the right occipital lobe. Brain Inj 13:213–216.

Miller R. 1991. Discovery and general behavioural correlates of the hippocampal theta rhythm. In Cortico-hippocampal interplay and the representation of contexts in the brain. (pp. 60–86). Springer Berlin Heidelberg.

Murray MM, Brunet D, Michel CM. 2008. Topographic ERP analyses: A step-by-step tutorial review. Brain Topogr 20:249–264.

Nadel L, Moscovitch M. 1997. Memory consolidation, retrograde amnesia and the hippocampal complex. Curr Opin Neurobiol 7: 217–227.

Nahum L, Gabriel D, Spinelli L, Momjian S, Seeck M, Michel CM, Schnider A. 2011. Rapid consolidation and the human hippocampus: Intracranial recordings confirm surface EEG. Hippocampus 21:689–693.

Nahum L, Pignat JM, Bouzerda-Wahlen A, Gabriel D, Liverani MC, Lazeyras F, Ptak R, Richiardi J, Haller S, Thorens G, Zullino DF, Guggisberg AG, Schnider A. 2014. Neural Correlate of Anterograde Amnesia in Wernicke-Korsakoff Syndrome. Brain Topogr 28: 760–770.

Raghavachari S, Lisman JE, Tully M, Madsen JR, Bromfield E, Kahana MJ. 2006. Theta oscillations in human cortex during a working-memory task: Evidence for local generators. J Neurophysiol 95:1630–1638.

Ranganath C, D'Esposito M. 2001. Medial temporal lobe activity associated with active maintenance of novel information. Neuron 31:865–873.

Sauseng P, Klimesch W, Schabus M, Doppelmayr M. 2005. Fronto-parietal EEG coherence in theta and upper alpha reflect central executive functions of working memory. Int J Psychophysiol 57: 97–103.

Sauseng P, Klimesch W, Heise KF, Gruber WR, Holz E, Karim AA, Glennon M, Gerloff C, Birbaumer N, Hummel FC. 2009. Brain oscillatory substrates of visual short-term memory capacity. Curr Biol 19:1846–1852.

Sekihara K, Nagarajan SS, Poeppel D, Marantz A. 2004. Performance of an MEG adaptive-beamformer source reconstruction technique in the presence of additive low-rank interference. IEEE Trans Biomed Eng 51:90–99.

Selden NR, Gitelman DR, Salamon-Murayama N, Parrish TB, Mesulam MM. 1998. Trajectories of cholinergic pathways within the cerebral hemispheres of the human brain. Brain 121 (Pt 12): 2249–2257.

Snodgrass JG, Vanderwart M. 1980. A standardized set of 260 pictures: Norms for name agreement, image agreement, familiarity, and visual complexity. J Exp Psychol Hum Learn 6: 174–215.

Spinelli L, Andino SG, Lantz G, Seeck M, Michel CM. 2000. Electromagnetic inverse solutions in anatomically constrained spherical head models. Brain Topogr 13:115–25.

Squire LR, Stark CE, Clark RE. 2004. The medial temporal lobe*. Annu Rev Neurosci 27:279–306.

Suzuki WA, Amaral DG. 1994. Perirhinal and parahippocampal cortices of the macaque monkey: Cortical afferents. J Comp Neurol 350:497–533.

Valenstein E, Bowers D, Verfaellie M, Heilman KM, Day A, Watson RT. 1987. Retrosplenial amnesia. Brain 110 (Pt 6):1631–1646.

Van Strien JW, Verkoeijen PP, Van der Meer N, Franken IH. 2007. Electrophysiological correlates of word repetition spacing: ERP and induced band power old/new effects with massed and spaced repetitions. Int J Psychophysiol 66:205–214.

Vilberg KL, Davachi L. 2013. Perirhinal-hippocampal connectivity during reactivation is a marker for object-based memory consolidation. Neuron 79:1232–1242.

Vilberg KL, Rugg MD. 2008. Memory retrieval and the parietal cortex: A review of evidence from a dual-process perspective. Neuropsychologia 46:1787–1799.

Wagner AD, Maril A, Schacter DL. 2000. Interactions between forms of memory: When priming hinders new episodic learning. J Cogn Neurosci 12 Suppl 2:52–60.

Xue G, Mei L, Chen C, Lu ZL, Poldrack R, Dong Q. 2011. Spaced learning enhances subsequent recognition memory by reducing neural repetition suppression. J Cogn Neurosci 23:1624–1633.